

Received 25 November 2023; revised 16 January 2024; accepted 23 January 2024. Date of publication 26 January 2024; date of current version 9 February 2024. The review of this article was arranged by Editor K. Cheng.

Digital Object Identifier 10.1109/JEDS.2024.3358830

Investigation of Photosensitive Polyimide With Low Coefficient of Thermal Expansion and Excellent Adhesion Strength for Advanced Packaging Applications

YUAN-CHIU HUANG¹, HAN-WEN HU¹, YUN-HSI LIU¹, HUI-CHING HSIEH²,
AND KUAN-NENG CHEN¹ (Fellow, IEEE)

¹ Institute of Electronics, National Yang Ming Chiao Tung University, Hsinchu 300, Taiwan
² LCY Chemical Corp., Kaohsiung 811, Taiwan

CORRESPONDING AUTHOR: K.-N. CHEN

This work was supported in part by the Semiconductor Research Corporation (SRC), the "Center for the advanced Semiconductor Technology Research" from the Featured Areas Research Center Program within the framework of the Higher Education Sprout Project by the Ministry of Education (MOE), Taiwan, and in part by the National Science and Technology Council, Taiwan, under Grant NSTC 112-2221-E-A49-163-MY3 and Grant NSTC 110-2221-E-A49-086-MY3.

ABSTRACT In advanced packaging schemes, such as fan-out integration technology, photosensitive polyimide (PSPI) is the key material to the fabrication of panel level redistribution-layer (RDL). However, a large mismatch of coefficient of thermal expansion (CTE) between silicon (Si) and PSPI will cause serious warpage issue. Furthermore, polyimide deformation may occur under external heat and pressure, leading to deterioration of RDL reliability. In this work, PSPI with low CTE and excellent adhesion strength on different substrate was developed and evaluated by lithography test, adhesion test, and reliability test, showing the high feasibility for the application in advanced packaging process.

INDEX TERMS Photosensitive polyimide, low CTE, adhesion enhancement, advanced packaging, RDL fabrication.

I. INTRODUCTION

As the dramatic growth of 5G, artificial intelligence (AI), and high-performance computing (HPC) markets, the demand for integration of chips with high bandwidth and short interconnect length has been a vast expansion [1], [2]. 2.5D interposer technology was developed to realize heterogeneous integration of memories and processors with high-bandwidth, high performance, low power consumption, and low RC delay. However, the use of Si interposer and through silicon via (TSV) technique in 2.5D packaging leads to the very high process cost [3]. Compared with 2.5D interposer technology, fan-out integration technology shows the great potential to provide multi-chips integration with high-speed communication and competitive cost. Accordingly, the fan-out integration packaging structure has been widely used in the applications of smart phones and power management ICs in recent years [4], [5].

In the fan-out process, panel-level RDL can be fabricated on molded chips (chip-first) or on carrier (chip-last), as shown in Fig. 1. With the use of PSPI as dielectric in RDL, which can define RDL pattern directly, the lithography process can be simplified. Nevertheless, in general case, the CTE of PI films in the film plane direction is ranging from 40 to 80 ppm/°C, but the CTE of metal is much lower about 17 ppm/°C for Cu foil. The large mismatch of CTE between metal substrates and PI films will cause serious warpage issue, leading to poor joint reliability [6], [7], [8]. In addition, polyimide deformation may occur to deteriorate the reliability of RDL under external heat and pressure. Accordingly, the development of PSPI with lower CTE and excellent adhesion strength has the potential to improve the reliability of PSPI-based RDL structure.

There are several approaches to reduce CTE. One promising method is the incorporation of amide groups in PIs [9], [10]. In this study, PSPI with low CTE and

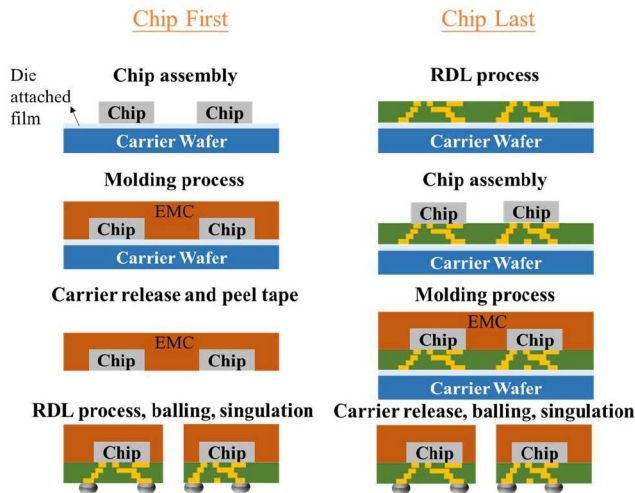


FIGURE 1. The schematic of fan-out process flow.

excellent adhesion strength have been developed by selection of appropriate precursor and photo-sensitive group. After preparation of PSPI, lithography test was performed to optimize concentration of photo-sensitive group to realize lithography pattern with good morphology. In addition, the adhesion of PSPI is an important factor for the applications of PSPI-based RDL structures.

Thus, adhesion of PSPI was investigated by four-point bending system for the substrates of Cu, Al, oxide, and nitride, which are commonly used metal and dielectric in the semiconductor industry. Furthermore, silane with different groups was added in PSPI to enhance its adhesion on different substrates. Finally, chemical resistance test and thermal cycling test (TCT) were conducted to examine the reliability of PSPI. Thus, the properties of PSPI developed in this work has been evaluated completely, showing the feasibility for the applications in advanced packaging structures.

II. EXPERIMENTAL PROCEDURE

A. PREPARATION OF MATERIALS

The characteristics of PSPI are mainly dominated by the material composition of the precursor. To obtain PSPI with low CTE, pyromellitic dianhydride (PMDA) structures, p-phenylenediamine (PPDA) or other rigid structure monomers were commonly selected as monomers of precursor due to the high rigidity, as shown in Fig. 2 [11].

The CTE measurement requires a sample was prepared by a 20- μm -thick layer of PSPI uniformly coated on a glass substrate. Following a hard baking process, this substrate is diced into 1 cm x 10 cm chips. These PSPI samples were then measured using a thermal mechanical analyzer (TMA) over a temperature range of 50 to 300 $^{\circ}\text{C}$. In this study, we developed a novel modified PSPI with a lower CTE compared to previous works, which was achieved by the addition of a photo-sensitive group. The comparison of thermal and mechanical properties of PSPI is shown in Table 1. After the preparation of the novel PSPI, lithography

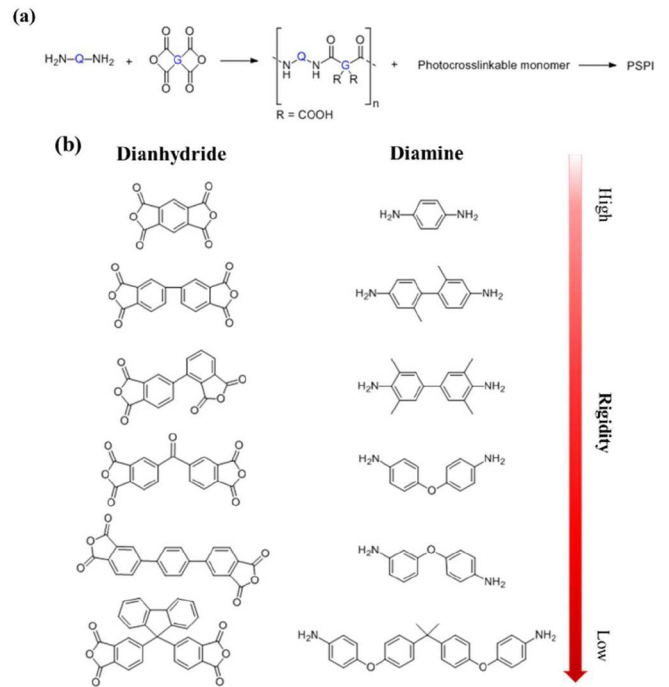


FIGURE 2. (a) The precursor of PSPI (b) selection of dianhydride or diamine with different rigidity.

test, adhesion test, chemical resistance test, and reliability test were performed in this study to verify the feasibility of PSPI in industrial applications.

B. FOUR-POINT BENDING SYSTEM

To evaluate adhesion of PSPI on different substrates, the method of four-point bending test was applied [12], [13], which is mainly composed of a stepper, a loading cell, and a sample holder. In the four-point bending, the sample fixed on the holder would be bended by the loading cell at a constant velocity (3 - 5 $\mu\text{m/s}$). Accordingly, the interfacial fracture energy (G_c value) can be calculated by a formulaic method:

$$G_c = \frac{21(1 - \nu^2)P_C^2 l^2}{16Eb^2h^3} \quad (1)$$

In this formula, ν is the Poisson's ratio of the silicon substrate; P_C is the loading force to the sample; l is the distance between inner and outer pins; E is the elastic modulus of the silicon substrate; b is the width of the sample; and h is the thickness of the single-sided silicon substrate. Based on the calculated quantitative data, the adhesion strength under different conditions can be compared.

C. SAMPLE PREPARATION FOR ADHESION TEST

Fig. 3 shows the schematic diagram of the cross-sectional structure for the bending test. In this study, the adhesion of PSPI on different materials was evaluated, including Cu, Al, SiO_2 , and SiN , which are the commonly used metals and dielectrics in the semiconductor industry. The

TABLE 1. Thermal and mechanical properties of PSPI.

		PSPI in this work	LT-6100 [15], [16]	LT-6600 [15], [16]	PDA-BPDA/6-FDA [17]
T _g	(°C)	284	160	194	350
CTE	(ppm/°C)	34	70	60	34
Curing Temperature	(°C)	280	200-250	200-250	250

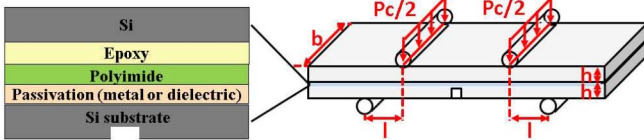


FIGURE 3. Cross-sectional view of the test structure for the four-point bending test.

process flow to prepare the sample for the measurements of the four-point bending test is shown in Fig. 4. RCA cleaned 4-inch Si wafer was used as the substrate, followed by thermal oxidation with thicknesses of 500 nm. Next, the layer of metal or dielectric was deposited by physical vapor deposition (PVD) or plasma-enhanced chemical vapor deposition (PECVD), and then PSPI was coated on it by the spin-coater. After coating of PSPI, soft baking, exposure, development, and hard baking were consecutively performed with the optimized parameters. Next, epoxy was coated on the sample by the spin coater with parameters of 3000 rpm for 10 seconds and 6000 rpm for 30 seconds, which can glue the sample with another Si wafer. Finally, the sample was diced into 7 cm × 0.3 cm pieces and sent for four-point bending measurements. Note that the sample was notched with 300 nm thickness to enable the breakage to occur in the middle of the sample during the bending test process.

III. RESULTS AND DISCUSSION

A. LITHOGRAPHY TEST OF PSPI

The PSPI was coated on a 4-inch Si wafer by a spin-coater for the lithography test. The optimized parameters to define the pattern of PSPI were described as follows. At first, the wafer with coated PSPI was soft-baked at 90 °C for 240 seconds on a hot plate. After a cool-down duration for 180 seconds, the exposure process of 150 mJ/cm² was performed using Aligner (AG1000-6N-ST), followed by post-exposure baking at 90 °C for 120 seconds. Next, the sample was developed by cyclopentanone and rinsed by propylene glycol monomethyl ether acetate (PGMEA) at room temperature to form the lithography pattern. After the lithography process, the sample was cured at 280 °C for 1 hour by the oven (Yotec, DH-400N) under N₂ atmosphere to complete the imidization of polyimide [14], [15].

The pattern capability of PSPI was verified by the SEM analyses, as shown in Fig. 5. Fig. 5(a) shows the high uniformity of lithography results in a large area, and Fig. 5(b) shows the enlarged cross-sectional view of the pattern with thickness of 10 μm and opening of 20 μm.

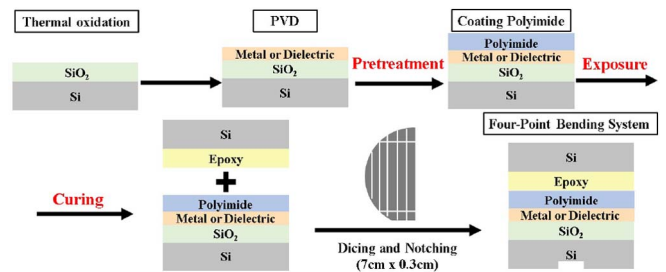


FIGURE 4. Schematic of the process flow of adhesion test.

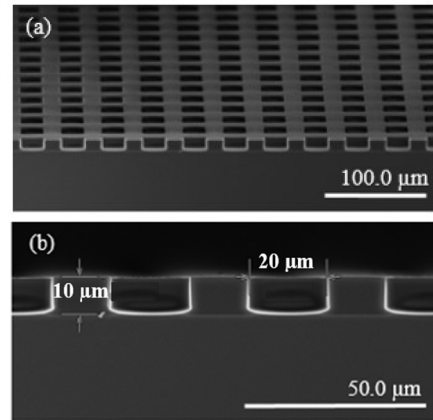


FIGURE 5. Pattern profile of PSPI (a) SEM image of cross-sectional view inspection after lithography with 20 μm hole. (b) drawing of partial enlargement of (a).

Openings above 20 μm pitch can be achieved with the excellent pattern profile using this PSPI.

B. ADHESION TEST ON DIFFERENT SUBSTRATE

After PSPI was cured at 280 °C to form polyimide, the adhesion of PSPI on Cu, Al, SiO₂, and SiN was measured by the four-point bending test, as shown in Fig. 6(a). Compared with the previous work [18], the adhesion of PSPI in this work on SiO₂ or SiN is better, while the adhesion of PSPI on the Cu substrate faces the peeling-off issue. To discuss this phenomenon, the adhesion of PSPI on Cu under different curing temperatures was measured, as shown in Fig. 6(b). It was observed that the adhesion of PSPI on the Cu substrate was increased with the rising curing temperature from room temperature to 230 °C. However, for the curing temperature of 280 °C, PSPI was peeled off from the Cu substrate. The PSPI peeling is due to poor adhesion between Cu and PI, compounded by the CTE mismatch which makes peeling between Cu and PI more likely. This issue arises because Cu and PI have different coefficients of thermal expansion (CTE), and the mismatch in CTE between these materials leads to increased stress as temperatures rise. Such stress can cause material deformation or the formation of stress concentrations, ultimately leading to defects like peeling or delamination [19], [20], [21]. To solve this issue, the pretreatment on the Cu surface was developed in this work.

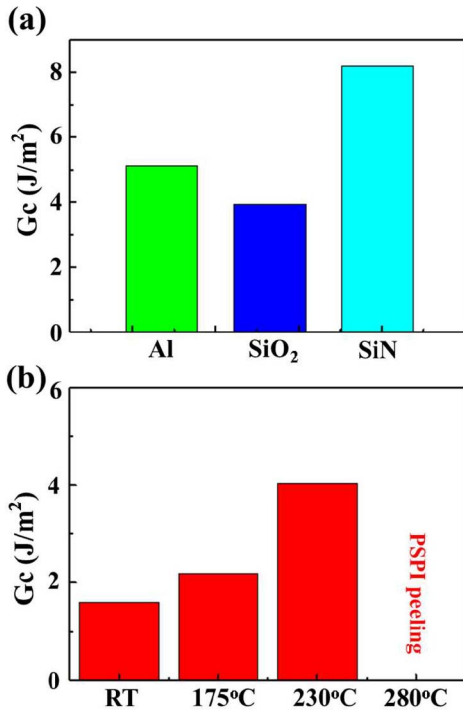


FIGURE 6. The adhesion strength (a) PSPI on different substrate (Al, SiO₂, SiN). (b) PSPI on Cu substrate was baked from room temperature to 280 °C.

TABLE 2. The surface roughness after O₂ plasma pretreatment.

Sample	Ra (nm)	Rq (nm)	Z-range (nm)
Without pretreatment	3.06	3.95	42.9
With 100 s plasma pretreatment	3.47	4.49	62
With 300 s plasma pretreatment	3.76	4.91	57
With 600 s plasma pretreatment	3.8	5.37	102

C. SURFACE PRETREATMENT

Since Cu is the excellent candidate as interconnect in RDL due to its outstanding conductivity and competitive cost [22], adhesion of PSPI on Cu is a critical factor for the industrial applications. Therefore, the pretreatment method was developed to enhance the adhesion strength of PSPI on the Cu substrate [23]. Aforementioned, PSPI was peeled off from the Cu substrate due to the rapid oxidation of Cu during the curing process. In this work, the pretreatment method by O₂ plasma was used to form the stable Cu oxides on the Cu surface before coating PSPI.

The atomic force microscope (AFM) analyses were performed to evaluate the surface roughness, as shown in Table 2 and Fig. 7 (a)–(d). For the sample without plasma pretreatment, the arithmetic average of absolute values of the surface height deviations (Ra) is 3.06 nm, and the root mean square average of height deviations (Rq) is 3.95 nm. With the plasma pretreatment for 100 seconds, 300 seconds, and 600 seconds, the Ra of the sample is slightly increased to 3.47 nm, 3.76 nm, and 3.80 nm, respectively.

After O₂ plasma pretreatment, a slight increase in the surface roughness of the polyimide is observed, with

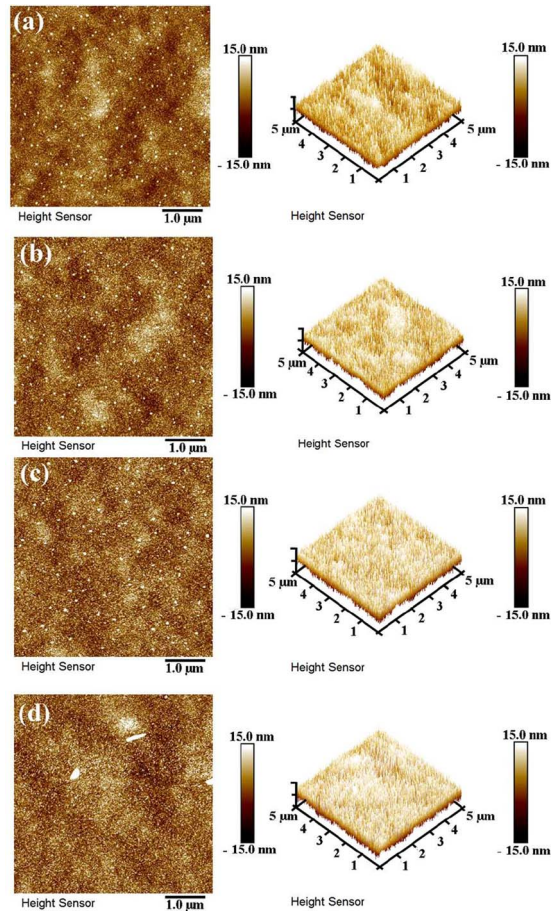


FIGURE 7. AFM results comparison of surface roughness between (a) before plasma pretreatment (b) after plasma pretreatment with plasma power 300 W for 100 seconds (c) after plasma pretreatment with plasma power 300 W for 300 seconds (d) after plasma pretreatment with plasma power 300 W for 600 seconds.

measurements indicating a marginal rise in both Ra and Rq values. Some research also mentions that an increase in plasma power, repeated plasma pretreatment, or extended duration of plasma pretreatment can potentially increase surface roughness [24], [25], [26]. Additionally, the plasma pretreatment significantly enhances the surface energy of the substrates. This increased surface energy is associated with a lower contact angle, indicating a more hydrophilic interface. This change can be attributed to the plasma’s ability to introduce polar functional groups, increasing the number of binding sites and thus improving wettability. Enhanced wettability is vital, allowing the polyimide to achieve more extensive contact with the substrate [27], [28], [29].

Numerous studies have demonstrated that plasma treatment of appropriate duration can significantly increase the hydrophilicity of the contact interface. To further validate this, contact angle measurements were performed under various conditions: plasma power at 300 W for durations of 100 seconds, 300 seconds, and 600 seconds. The results, as shown in Fig. 8 (a), indicate a substantial reduction in contact angle regardless of the condition, following the

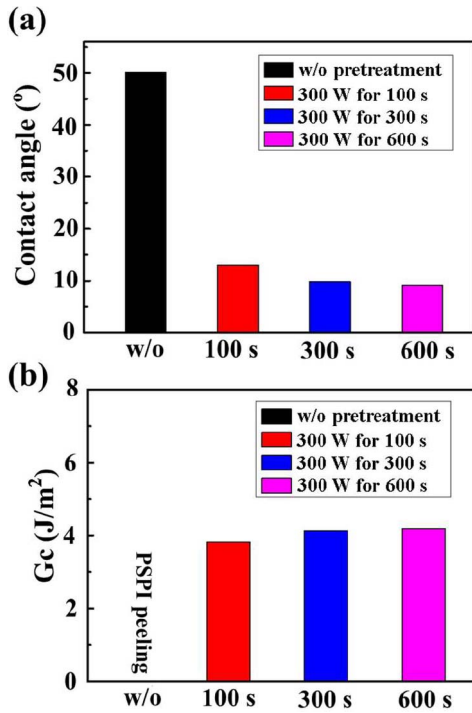


FIGURE 8. (a) Contact angle measurement results of PSPI before plasma pretreatment and after plasma treatment (b) adhesion strength after plasma pretreatment and after plasma treatment.

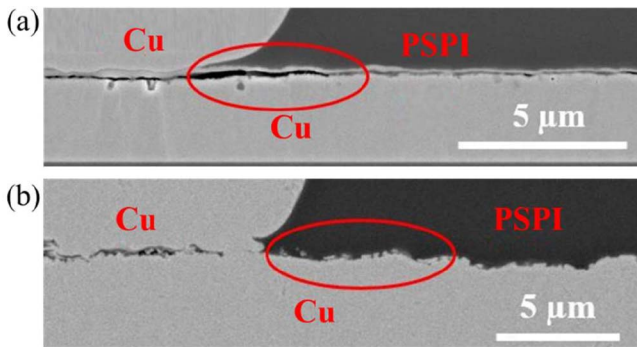


FIGURE 9. SEM cross-section image of RDL fabrication with PSPI (a) without pretreatment (b) with plasma pretreatment.

O₂ plasma pretreatment. Moreover, it was observed that without any additional adhesion promoter, the O₂ plasma pretreatment can significantly enhance the adhesion strength, as shown in Fig. 8 (b). O₂ plasma pretreatment thus ensures optimal adhesion strength, securing a reliable polyimide/Cu interface for industrial applications.

Many researches show that plasma treatment of proper duration can make the contact interface to be more hydrophilic [30], [31]. For packaging application, the fabrication of RDL using PSPI has been demonstrated in Fig. 9 (a) and (b). Without plasma pretreatment, peeling and cracking issue was observed at the interface between Cu and PSPI. After plasma pretreatment, the better adhesion interface between Cu and PSPI can be obtained. Furthermore,

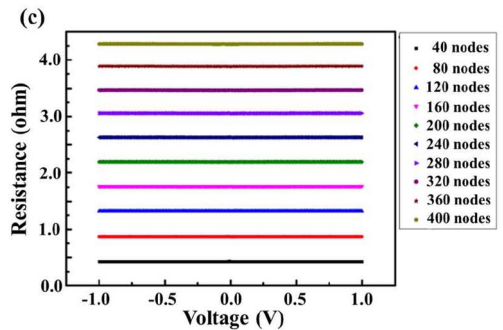
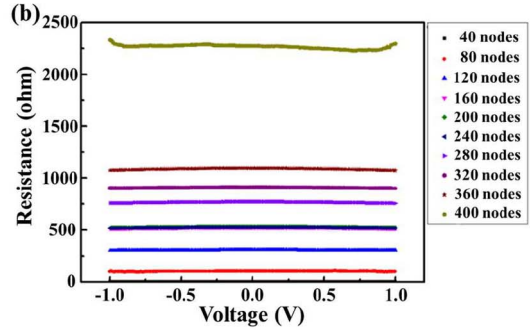
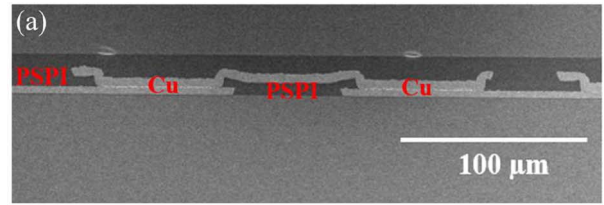


FIGURE 10. (a) SEM cross-section image of contact nodes (b) electrical measurement without plasma pretreatment (c) electrical measurement with plasma pretreatment.

the daisy chain structure has been designed with 40 to 400 contact nodes and 60 × 60 μm contact area of each node for electrical measurements of the PSPI based RDL samples. The cross-section SEM image of the contact nodes is shown in Fig. 10 (a), and the results of electrical measurements of samples without plasma pretreatment and with plasma pretreatment are shown in Fig. 10 (b) and Fig. 10 (c). Accordingly, the series resistance can be decreased significantly and become more stable after plasma pretreatment, verifying that plasma pretreatment can not only remove the residue between the first layer of Cu and a second layer of Cu but also effectively increase the adhesion strength between Cu and PSPI.

D. ADDITION TO IMPROVE ADHESION STRENGTH OF PSPI

In previous research, the addition of silane coupling agents has been shown to improve the adhesion of polyimide to inorganic substrates [32], [33]. We explored various silane coupling agents, such as epoxy and phosphoric ester groups, to enhance the bond between polyimide and different substrates. These agents facilitate reactive sites for robust chemical bonding, as demonstrated the samples A-E in

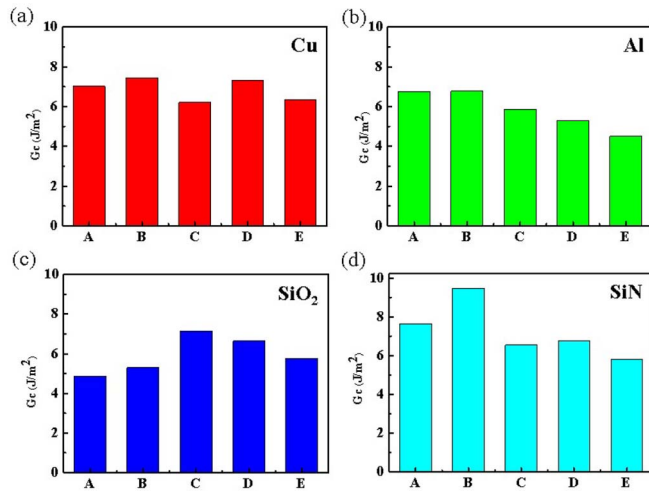


FIGURE 11. Adhesion of PSPI with different additive on different materials (a) Cu, (b) Al, (c) SiO₂, (d) SiN.

Fig. 11, each with a distinct silane agent. Further supporting our findings, previous studies have emphasized the role of surface modifications in adhesion strength. For instance, PI surfaces treated with amine solutions exhibited optimal adhesion at specific drying temperatures, linked to the molecular weight of the amines [34]. Additionally, a study combining peel tests and density functional theory (DFT) simulations revealed aminoethyl-aminopropyltrimethoxysilane (AEAPS) as an effective silane agent for Cu adhesion, supported by high adhesion energy and peel strength findings [29]. These insights align with our observations in Fig. 11 (a)–(d), where silane coupling agents significantly improve PSPI adhesion strength.

E. RELIABILITY TEST

The fabrication of a PSPI-based RDL structure involves an etching process with different chemical solvents. Thus, chemical resistance test is important for the development of PSPI. In this work, the commonly used organic solvent, PR stripper, alkaline, and etchant were selected for chemical resistance test, such as NMP, PGMEA, Acetone, SNT-35, PRS-3000 (Avantor), nitric acid, sulfuric acid, hydrofluoric acid, Titanium etchant. After soaking the sample in different chemical solution at room temperature for 5 minutes and 25 minutes, the morphology and film thickness of PSPI was investigated by the analyses of SEM. The results of the chemical resistance test, as shown in Table 3, indicate that the variation of film thickness is minimal, demonstrating the excellent chemical resistance of PSPI.

In addition, a thermal cycling test (TCT) was performed to verify the thermal stability of this modified PSPI. Following the standard of JESD22-A104B, a single loop of TCT includes rising up and cooling down of temperature from -55 °C to 125 °C at a 15 °C/min ramping rate. Fig. 12 (a) indicates PSPI can maintain its adhesive strength on materials of Cu, Al, SiN, SiO₂, and PSPI (PSPI on PSPI)

TABLE 3. The results of chemical resistance test.

	Solution Item	Test Temp. (°C)	Test Time (min)	thickness change (%)
Metal etchant	Nitric acid 30%	Room temperature	5	0.39 %
			25	1.18 %
	Sulfuric acid 30%	Room temperature	5	0.78 %
			25	1.42 %
	HF 1%	Room temperature	5	0.27 %
			25	0.51 %
Ti etchant	Room temperature	5	1.60 %	
		25	0.44 %	
Organic solvent	NMP	Room temperature	5	2.58%
			25	2.58%
	PGMEA	Room temperature	5	4.09%
			25	1.19%
	Acetone	Room temperature	5	3.50%
			25	3.96%
PR stripper	SNT-35	Room temperature	5	2.14%
			25	1.38%

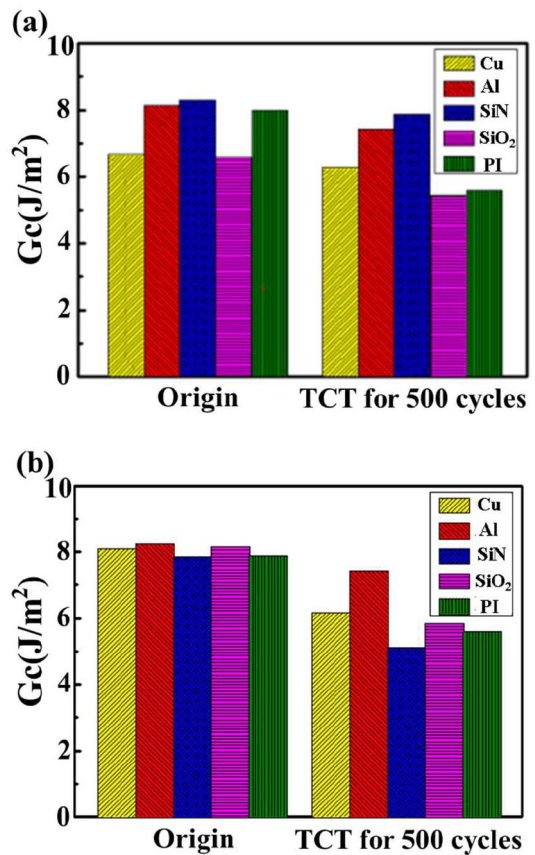


FIGURE 12. TCT results of (a) PSPI on different materials (b) commercial PSPI on different materials.

before and after TCT for 500 cycles. As shown in Fig. 12 (b), commercial PSPI samples before and after TCT for 500 cycles have been fabricated and investigated. Compared with this commercial PSPI, the adhesion strength of PSPI in this work has a high feasibility for industrial applications.

IV. CONCLUSION

PSPI has been the key material in advanced packaging applications, such as the fabrication of RDL in fan-out

integration packaging, due to the simplified lithography process. However, the large CTE mismatch induces serious warpage issues. Thus, the novel PSPI with low CTE and excellent adhesion strength was developed in this work by a selection of monomers with higher rigidity. To demonstrate the feasibility of this PSPI in advanced packaging applications, a lithography test, adhesion test, and reliability test were consecutively performed.

With the optimized lithography parameters, the excellent pattern capability of PSPI can be validated for both square and circle opening of 15 μm . The adhesion strength between PSPI and different materials has been evaluated by the four-point bending system, including Cu, Al, SiO₂ and SiN. Note that the adhesion of PSPI on the Cu substrate is challenged by the rapid oxidation of Cu during the curing process, which can be solved by the pretreatment of hot plate heating and O₂ plasma. The O₂ plasma pretreatment at 300 W for 300 seconds were verified as the better parameter to improve adhesion strength, reduce surface roughness, and decrease series resistance significantly. Furthermore, the addition of a silane coupling agent with different structures was investigated to enhance the adhesion of PSPI. It was observed that the addition of silane with the different silane coupling agent can provide higher adhesion strength. Finally, PSPI can pass the chemical resistance test and TCT with negligible change of properties, showing that PSPI developed in this work has great potential in industrial applications to provide advanced packaging structures with higher reliability due to its lower CTE and excellent adhesion strength.

REFERENCES

- [1] M. F. Chen et al., "SoIC for low-temperature, multilayer 3D memory integration," in *Proc. IEEE 70th Electron. Compon. Technol. Conf. (ECTC)*, 2020, pp. 855–860, doi: [10.1109/ECTC32862.2020.00139](https://doi.org/10.1109/ECTC32862.2020.00139).
- [2] H. Sakakibara et al., "Advanced plating photoresist development for advanced IC packages," in *Proc. 16th Int. Conf. Electron. Packag. Technol. (ICEPT)*, 2015, pp. 1348–1351, doi: [10.1109/ICEPT.2015.7236828](https://doi.org/10.1109/ICEPT.2015.7236828).
- [3] N. Chang et al., "3D micro bump interface enabling top die interconnect to true circuit through silicon via wafer," in *Proc. IEEE 70th Electron. Compon. Technol. Conf. (ECTC)*, 2020, pp. 1888–1893, doi: [10.1109/ECTC32862.2020.00295](https://doi.org/10.1109/ECTC32862.2020.00295).
- [4] J. H. Lau, *Semiconductor Advanced Packaging*. Singapore: Springer, 2021, doi: [10.1007/978-981-16-1376-0_1](https://doi.org/10.1007/978-981-16-1376-0_1).
- [5] S. W. Yoon, J. A. Caparas, Y. Lin, and P. C. Marimuthu, "Advanced low profile PoP solution with embedded wafer level PoP (eWLB-PoP) technology," in *Proc. IEEE 62nd Electron. Compon. Technol. Conf.*, 2012, pp. 1250–1254, doi: [10.1109/ECTC.2012.6248995](https://doi.org/10.1109/ECTC.2012.6248995).
- [6] M. Brunnbauer et al., "An embedded device technology based on a molded reconfigured wafer," in *Proc. 56th Electron. Compon. Technol. Conf.*, 2006, pp. 1–5, doi: [10.1109/ECTC.2006.1645702](https://doi.org/10.1109/ECTC.2006.1645702).
- [7] H. Araki et al., "Fabrication of redistribution structure using highly reliable photosensitive Polyimide for fan out panel level packages," in *Proc. Int. Wafer Level Packag. Conf. (IWLPC)*, 2018, pp. 1–6, doi: [10.23919/IWLPC.2018.8573286](https://doi.org/10.23919/IWLPC.2018.8573286).
- [8] M. Hasegawa and S. Horii, "Low-CTE polyimides derived from 2,3,6,7-naphthalenetetracarboxylic dianhydride," *Polymer J.*, vol. 39, no. 6, pp. 610–621, 2007, doi: [10.1295/polymj.PJ2006234](https://doi.org/10.1295/polymj.PJ2006234).
- [9] G. Qian et al., "Polyimides with low coefficient of thermal expansion derived from diamines containing benzimidazole and amide: Synthesis, properties, and the N-substitution effect," *J. Polymer Sci.*, vol. 59, no. 6, pp. 510–518, 2021, doi: [10.1002/pol.20200879](https://doi.org/10.1002/pol.20200879).
- [10] M. Hasegawa, "Development of solution-processable, optically transparent polyimides with ultra-low linear coefficients of thermal expansion," *Polymers*, vol. 9, no. 10, p. 520, 2017, doi: [10.3390/polym9100520](https://doi.org/10.3390/polym9100520).
- [11] S. Xi, X. Wang, Z. Zhang, T. Liu, X. Zhang, and J. Shen, "Influence of diamine rigidity and dianhydride rigidity on the microstructure, thermal and mechanical properties of cross-linked polyimide aerogels," *J. Porous Mater.*, vol. 28, no. 3, pp. 717–725, 2021, doi: [10.1007/s10934-020-01028-2](https://doi.org/10.1007/s10934-020-01028-2).
- [12] H.-J. Sue and A. F. Yee, "Study of fracture mechanisms of multiphase polymers using the double-notch four-point-bending method," *J. Mater. Sci.*, vol. 28, no. 11, pp. 2975–2980, 1993, doi: [10.1007/BF00354702](https://doi.org/10.1007/BF00354702).
- [13] M. P. Hughey et al., "Four-point bend Adhesion measurements of copper and permalloy systems," *Eng. Fracture Mech.*, vol. 71, no. 2, pp. 245–261, 2004, doi: [10.1016/S0013-7944\(03\)00100-0](https://doi.org/10.1016/S0013-7944(03)00100-0).
- [14] T. Yuba, R. Okuda, M. Tomikawa, and J. H. Kim, "Soft baking effect on lithographic performance by positive tone photosensitive polyimide," *J. Photopolym. Sci. Technol.*, vol. 23, no. 6, pp. 775–779, 2010, doi: [10.2494/photopolymer.23.775](https://doi.org/10.2494/photopolymer.23.775).
- [15] M. Tomikawa, R. Okuda, and H. Ohnishi, "Photosensitive polyimide for packaging applications," *J. Photopolym. Sci. Technol.*, vol. 28, no. 1, pp. 73–77, 2015, doi: [10.2494/photopolymer.28.73](https://doi.org/10.2494/photopolymer.28.73).
- [16] Y. Shoji, Y. Masuda, K. Hashimoto, K. Isobe, Y. Koyama, and R. Okuda, "Development of novel low-temperature curable positive-tone photosensitive dielectric materials with high elongation," in *Proc. IEEE 66th Electron. Compon. Technol. Conf. (ECTC)*, 2016, pp. 1707–1712, doi: [10.1109/ECTC.2016.149](https://doi.org/10.1109/ECTC.2016.149).
- [17] L. Y. Tseng et al., "Alkaline-developable and negative-type photosensitive polyimide with high sensitivity and excellent mechanical properties using photo-base generator," *J. Polym. Sci.*, vol. 58, no. 17, pp. 2366–2375, 2020, doi: [10.1002/pol.20200409](https://doi.org/10.1002/pol.20200409).
- [18] C. H. Lu, Y. T. Kho, C. P. Chen, B. L. Tsai, and K. N. Chen, "Adhesion and material properties between polyimide and passivation layers for polymer/metal hybrid bonding in 3-D integration," *IEEE Trans. Compon., Packag. Manuf. Technol.*, vol. 9, no. 3, pp. 412–418, Mar. 2019, doi: [10.1109/TCPMT.2019.2895515](https://doi.org/10.1109/TCPMT.2019.2895515).
- [19] H. Li, G. Cheng, G. Xu, and L. Luo, "Influence of polyimide on thermal stress evolution in polyimide/Cu thick film composite," *J. Mater. Sci. Mater. Electron.*, vol. 27, no. 8, pp. 8325–8331, Aug. 2016, doi: [10.1007/s10854-016-4841-6](https://doi.org/10.1007/s10854-016-4841-6).
- [20] R. Jensen, J. Cummings, and H. Vora, "Copper/polyimide materials system for high performance packaging," *IEEE Trans. Comp., Hybrids, Manuf. Technol.*, vol. 7, no. 4, pp. 384–393, Dec. 1984, doi: [10.1109/TCHMT.1984.1136378](https://doi.org/10.1109/TCHMT.1984.1136378).
- [21] C. Zhu, W. Ning, G. Xu, and L. Luo, "Stress evolution during thermal cycling of copper/polyimide layered structures," *Mater. Sci. Semicond. Process.*, vol. 27, pp. 819–826, Nov. 2014, doi: [10.1016/j.mssp.2014.08.022](https://doi.org/10.1016/j.mssp.2014.08.022).
- [22] N. Inagaki, S. Tasaka, and T. Baba, "Surface modification of polyimide film surface by silane coupling reactions for copper metallization," *J. Adhes. Sci. Technol.*, vol. 15, no. 7, pp. 749–762, 2001, doi: [10.1163/15685610152540821](https://doi.org/10.1163/15685610152540821).
- [23] Y. I. Lee and Y. H. Choa, "Adhesion enhancement of ink-jet printed conductive copper patterns on a flexible substrate," *J. Mater. Chem.*, vol. 22, no. 25, pp. 12517–12522, 2012, doi: [10.1039/C2JM31381B](https://doi.org/10.1039/C2JM31381B).
- [24] U. Cvelbar, S. Pejovnik, M. Mozetič, and A. Zalar, "Increased surface roughness by oxygen plasma treatment of graphite/polymer composite," *Appl. Surface Sci.*, vol. 210, nos. 3–4, pp. 255–261, Apr. 2003, doi: [10.1016/S0169-4332\(02\)01286-2](https://doi.org/10.1016/S0169-4332(02)01286-2).
- [25] S.-J. Cho, J.-W. Choi, I.-S. Bae, T. Nguyen, and J.-H. Boo, "Surface plasma treatment of polyimide film for Cu metallization," *Jpn. J. Appl. Phys.*, vol. 50, no. 1, Jan. 2011, Art. no. 01AK02, doi: [10.1143/JJAP.50.01AK02](https://doi.org/10.1143/JJAP.50.01AK02).
- [26] S. H. Kim, S. W. Na, N.-E. Lee, Y. W. Nam, and Y.-H. Kim, "Effect of surface roughness on the Adhes. properties of Cu/Cr films on polyimide substrate treated by inductively coupled oxygen plasma," *Surface Coatings Technol.*, vol. 200, no. 7, pp. 2072–2079, Dec. 2005, doi: [10.1016/j.surfcoat.2005.05.021](https://doi.org/10.1016/j.surfcoat.2005.05.021).

- [27] J. S. Eom and S. H. Kim, "Plasma surface treatment of polyimide for adhesive Cu/80Ni20Cr/PI flexible copper clad laminate," *Thin Solid Films*, vol. 516, no. 14, pp. 4530–4534, May 2008, doi: [10.1016/j.tsf.2008.01.022](https://doi.org/10.1016/j.tsf.2008.01.022).
- [28] D. Wojcieszak, A. Ponedzialek, M. Mazur, J. Domaradzki, D. Kaczmarek, and J. Dora, "Influence of plasma treatment on wettability and scratch resistance of Ag-coated polymer substrates," *Mater. Sci. Poland*, vol. 34, no. 2, pp. 418–426, Jun. 2016, doi: [10.1515/msp-2016-0058](https://doi.org/10.1515/msp-2016-0058).
- [29] M. Miyazaki, Y. Kanegae, and T. Iwasaki, "Adhesion analysis of silane coupling agent/copper interface with density functional theory," *Mech. Eng. J.*, vol. 1, no. 4, pp. 1–10, 2014, doi: [10.1299/mej.2014smm0032](https://doi.org/10.1299/mej.2014smm0032).
- [30] N. Encinas, R. Dillingham, B. Oakley, J. Abenojar, M. Martínez, and M. Pantoja, "Atmospheric pressure plasma hydrophilic modification of a silicone surface," *J. Adhes.*, vol. 88, no. 4–6, pp. 321–336, 2012, doi: [10.1080/00218464.2012.659994](https://doi.org/10.1080/00218464.2012.659994).
- [31] S.-J. Cho, T. Nguyen, and J.-H. Boo, "Polyimide surface modification by using microwave plasma for Adhesion enhancement of Cu electroless plating," *J. Nanosci. Nanotechnol.*, vol. 11, no. 6, pp. 5328–5333, 2011, doi: [10.1166/jnn.2011.3793](https://doi.org/10.1166/jnn.2011.3793).
- [32] C. Xiao, D. Li, D. Zeng, F. Lang, Y. Xiang, and Y. Lin, "A comparative investigation on different silane coupling agents modified sericite mica/polyimide composites prepared by in situ polymerization," *Polym. Bull.*, vol. 78, no. 2, pp. 863–883, 2021, doi: [10.1007/s00289-020-03143-1](https://doi.org/10.1007/s00289-020-03143-1).
- [33] S. Babanzadeh, A. R. Mahjoub, and S. Mehdipour-Ataei, "Novel soluble thermally stable silane-containing aromatic polyimides with reduced dielectric constant," *Polym. Degradat. Stabil.*, vol. 95, no. 12, pp. 2492–2498, 2010, doi: [10.1016/j.polymdegradstab.2010.08.001](https://doi.org/10.1016/j.polymdegradstab.2010.08.001).
- [34] H. K. Yun et al., "Adhesion improvement of epoxy resin/polyimide joints by amine treatment of polyimide surface," *Polymer*, vol. 38, no. 4, pp. 827–834, Feb. 1997, doi: [10.1016/S0032-3861\(96\)00592-7](https://doi.org/10.1016/S0032-3861(96)00592-7).